C.P. No. 787

C.P. No. 787

MINISTRY OF AVIATION

AERONAUTICAL RESEARCH COUNCIL

CURRENT PAPERS

# Effects of Varied Loading Paths on Fatigue Endurances

## Part II - Some Load Fatigue Properties of H46 at Room Temperature

By

G.P. Tilly

LONDON: HER MAJESTY'S STATIONERY OFFICE

1965

SIX SHILLINGS NET

U.D.C. No. 539.431:669.15-194.57

C.P. No.787

March, 1964

# Effects of varied loading paths on fatigue endurances Part II - Some load fatigue properties of H46 at room temperature

- by -

G. P. Tilly

## SUMMARY

The constant load amplitude fatigue properties of an 11 per cent Cr-Mo-V-Nb steel (H46), have been examined at frequencies of 7 c/hr, 10 c/min and 8000 c/min at room temperature for repeated tension and push/pull loading.

Ductile type fractures were observed at very high stresses and brittle type fractures at less high stresses. The fracture types contained regions of both intercrystalline and transcrystalline failure together with numerous intercrystalline sub-cracks behind the fractures. The push/pull and the repeated tension stress/cycles to failure (S/N) fatigue curves converged to the static ultimate tensile strength at high stresses. Variations in the cyclic strain ranges of the different tests were examined and discussed in terms of the Bauschinger effect. The very high stress repeated tension tests at frequencies of 7 c/hr and 10 c/min exhibited a creep type time-dependent failure condition, whereas less high stresses tended to the more common room temperature cycle-dependent fatigue condition. For all testing conditions, the general trend was for higher frequencies to give greater numbers of cycles to failure at equivalent stresses and loading paths.

---

Replaces N.G.T.E. Memo. No.M.381 - A.R.C.26 055.

CONTENTS

| | | Page |
|---|---|---|
| 1.0 | Introduction | 4 |
| 2.0 | Material | 4 |
| 3.0 | Test-piece | 4 |
| 4.0 | Experimental | 5 |
| | 4.1 Technique | 5 |
| | 4.2 Programme | 5 |
| 5.0 | The repeated tension tests | 5 |
| 6.0 | The push/pull tests | 5 |
| 7.0 | Fracture types | 6 |
| 8.0 | Metallographic examinations | 6 |
| 9.0 | Strain-time records | 7 |
| | 9.1 Repeated tension strain records | 7 |
| | 9.2 Push/pull strain records | 7 |
| 10.0 | Discussion | 8 |
| 11.0 | Conclusions | 10 |
| Acknowledgements | | 11 |
| Notation | | 12 |
| References | | 13 |

Detachable Abstract Cards

TABLE

| No. | Title | |
|---|---|---|
| I | Constant load amplitude fatigue test results on H46 steel at room temperature | 14 |

APPENDIX

| No. | Title | |
|---|---|---|
| I | The diametral extensometer | 16 |

## ILLUSTRATIONS


| Fig. No. | Title |
|---|---|
| 1 | Constant load amplitude: Room temperature fatigue tests on H46: repeated tension S/t |
| 2 | Constant load amplitude: Room temperature fatigue tests on H46: repeated tension S/N |
| 3 | Constant load amplitude: Room temperature fatigue tests on H46: push/pull S/t |
| 4 | Constant load amplitude: Room temperature fatigue tests on H46: push/pull S/N |
| 5 | Ductile fracture and metallographic section |
| 6 | Brittle fracture and metallographic section |
| 7 | Ductile and brittle metallographic sections |
| 8 | Some cumulative strain/time curves for room temperature fatigue of H46 |
| 9 | Some diametral deformation - time records: Constant load amplitude fatigue of H46 |
| 10 | Views of the diametral extensometer assembly |

## 1.0 Introduction

The tests reported in this paper are essentially an individual section of an overall investigation into some of the effects of varied fatigue loading paths on life to failure of high temperature materials. The overall programme is intended to cover a large range of testing conditions from room temperature to typical maximum operating temperatures, and has been previously described in some detail[1]. This Memorandum describes constant load amplitude room temperature fatigue tests on H46 and will be followed by similar investigations at 400, 600, and 700°C for constant stress as well as constant load amplitude fatigue.

## 2.0 Material

The material tested was a vacuum cast H46 steel supplied as a 13 in. diameter forging. Blanks $\frac{5}{8}$ in. square in section were slit out in a longitudinal direction and heat treated at 1150°C for 30 min and air cooled, followed by 3 hr at 640°C and air cooled to give a hardness value within the range of 351 to 357 V.P.N.

The chemical composition was:-

| | | | | |
|---|---|---|---|---|
| Carbon | 0.18 | to | 0.20 | per cent |
| Manganese | 0.79 | | 0.90 | |
| Silicon | 0.28 | | 0.33 | |
| Sulphur | 0.016 | | 0.019 | |
| Phosphorus | 0.013 | | 0.017 | |
| Nickel | 0.78 | | 0.88 | |
| Chromium | 11.0 | | 11.4 | |
| Vanadium | 0.38 | | 0.41 | |
| Niobium | 0.24 | | 0.30 | |
| Molybdenum | 0.55 | | 0.64 | |
| Boron | 0.0035 | | 0.0040 | |
| Iron | | Balance | | |

## 3.0 Test-piece

A general standardised test-piece[2] with a 0.555 in. gauge length of 0.140 in. nominal diameter was used. The test section was surface ground to a finish of 8 micro-inches and polished circumferentially with 000 emery paper.

## 4.0 Experimental

### 4.1 Technique

The tests were conducted on a specially modified 10 ton Amsler Vibrophore machine, capable of applying both high frequency and low frequency fatigue loads. The experimental technique has been described previously[1]. An extensometer was designed and built for recording the diametral strain and is described in Appendix I.

### 4.2 Programme

Constant load amplitude fatigue tests were applied at nominal applied frequencies of 7 c/hr, 10 c/min* and 8000 c/min for both repeated tension and push/pull loading respectively. The diametral extensometer became operative at a late stage of the investigation and strain-time records were made of a representative selection of the tests.

## 5.0 The repeated tension tests

The fatigue results were expressed in the form of stress/time (S/t) curves (Figures 1 and 3) and the more common stress/number of cycles to failure (S/N) curves (Figures 2 and 4). It was clear from the repeated tension tests (Figures 1 and 2) that there were two distinct regions in the fatigue curve: a very high stress region where the slope was very small, and a lower stress region of steeper slope. The slowest frequency tests (7 c/hr) gave results that were on the low slope for test durations of up to 143 hr duration whilst the 10 c/min tests gave an initial region of low slope, followed by a region of markedly increased slope at around 5.5 hr to failure. The values of static ultimate tensile strength (U.T.S.) established by several replicate tests at speeds corresponding to 7 c/hr and 10 c/min were 70.5 ton/in$^2$ and 72.5 ton/in$^2$ respectively. It appeared that for failures in less than 5.75 hr duration the 10 c/min frequency gave superior endurances (as measured by time to failure) whereas for times greater than 5.75 hr the lower applied frequencies gave longer endurances. The 8000 c/min test data appeared to have an inherently higher experimental scatter than the lower frequency tests. The test points appeared to be best described by a convex curve similar to that normally associated with the presence of an endurance limit. The more familiar S/N plot (Figure 2) also illustrated the two regions of fatigue characterised by different slopes and indicated that there was an appreciable speed effect in terms of cycles to failure. There was a well defined transition between the two regions at around $10^4$ cycles to failure. The order of decreasing strength in terms of the frequencies was 8000 c/min, 10 c/min, and 7 c/hr, i.e., higher frequencies gave longer endurances for a given applied stress.

## 6.0 The push/pull tests

The push/pull test results, (Figures 3 and 4) did not exhibit the well defined fatigue regions that were exhibited by the repeated tension tests and the data at the three frequencies gave smooth S/t and S/N curves with no marked changes in slope. The speed effect was similar to that of the repeated tension tests with increasing frequency giving superior

* The 7 c/hr and 10 c/min fatigue cycles were applied at constant loading rates in terms of ton/min. The quoted frequencies were thus nominal values and the push/pull and repeated tension frequencies could vary by a factor of two for the same maximum applied stresses.

endurances as evinced by the 7 c/hr and 10 c/min tests over comparable stress ranges. The values of U.T.S. could be joined on to the 7 c/hr and 10 c/min S/N curves at the corresponding testing speeds (Figure 4) and the stress-wise separation of the two curves was equal to the differences in U.T.S. by virtue of the static speed effect. The 8000 c/min tests were not so readily comparable since they were conducted over a lower range of stresses and the region of overlap on the S/N diagram was very limited. (It was impracticable to fail the specimens at low numbers of cycles to failure for such high frequencies and no apparatus was available for making a static tensile test at a rate comparable to $1.2 \times 10^6$ t.s.i./min.)

## 7.0 Fracture types

Two classes of fracture resulted from the fatigue tests; ductile fractures at high stresses similar to delayed static fractures previously reported in other low cycle fatigue investigations[3], and low ductility fractures of brittle appearance at lower stresses. The changeover from the ductile to brittle types appeared to vary with the testing conditions. In the case of the repeated tension tests at a frequency of 7 c/hr (confined to high stresses) no brittle failures resulted whereas the 10 c/min fractures were ductile in appearance above 70.5 ton/in$^2$ and brittle below, with the brittle failures all associated with the region of steeper slope (low stress) on the fatigue curve. The 8000 c/min tests were brittle below 67.5 ton/in$^2$ but there was no marked change in slope at the changeover point. The push/pull tests exhibited a similar change in fracture type, those at the 7 c/hr tests being entirely ductile, and the 10 c/min tests being ductile above 65 ton/in$^2$ and brittle below. The 8000 c/min tests were ductile above 39 ton/in$^2$ and brittle below. In no case was there any obvious reason why the change in fracture appearance had taken place and the only common features were that for both repeated tension and push/pull loading the ductile fractures were confined to higher stresses. The fracture changeover point varied for each frequency and stress ratio. No brittle fractures resulted from the 7 c/hr tests under either repeated tension or push/pull loading up to 143 hr duration.

## 8.0 Metallographic examinations

Metallographic examinations revealed that the ductile type fractures were highly deformed close to the fracture surface and contained deep fissures parallel to the testing direction (Figure 5). The fractures were predominantly transcrystalline, although there was some evidence of isolated areas of intercrystalline failure even on the $\frac{1}{2}$ cycle static fractures. There were a number of intercrystalline cavities behind the fracture surface, and in addition, the fissures leading into the fractures also appeared to be basically intercrystalline (Figure 7.1). The brittle type fractures had a macroscopic 'crystalline' appearance with bright clear facets and a very fine structure similar to that of the brittle fracture of mild steel. The microscopic examination at X500 magnification of sections taken perpendicular to the test direction, showed that the brittle type fracture surfaces were comparatively smooth and there were no deep fissures or heavy deformation present as in the ductile type fractures. The brittle fracture mode appeared to be mostly intercrystalline although there were many regions of transcrystalline cracking (Figure 6.2). The bright facets were very similar to cleavage planes although there were no characteristic river patterns apparent at X500 magnifications. Treatment with Fry's reagent was negative. (Tests have been reported in which Fry's reagent was used to produce dislocation etch pits on ferrite; it was hoped that a similar treatment would produce an etch pit structure on the brittle facets of the H46 if they were indeed (100) cleavage planes.) Some of the lower stress brittle type fractures had what appeared to be a 'thumbnail' fatigue initiation, although there was no clear cut fatigue topography and this region might have been equally well classified as being of creep appearance. There appeared to be no essential differences between the repeated tension and the push/pull test failures. Both exhibited deep intercrystalline fissures in the ductile type failures and were part intercrystalline part transcrystalline (Figure 7).

## 9.0 Strain-time records

### 9.1 Repeated tension strain records

Continuous diametral strain-time records were made during the tests and were analysed in terms of total accumulated strain and cyclic strain range. In the case of the repeated tension tests it appeared that the strain accumulated during the test according to laws similar to those that describe conventional steady load creep deformation and confirmed the general trends reported for constant stress amplitude fatigue tests by Landau[4]. There were well defined primary, secondary and tertiary stages during which the accumulated fatigue strain initially increased rapidly, attained a more or less constant rate and finally increased again very rapidly immediately prior to fracture (Figure 8.1). The tertiary stage was most marked on the records of tests that resulted in ductile type fractures, and was either abbreviated or was not reached at all in the case of the brittle type fractures. The steady state secondary stage was most marked in the long endurance tests but was almost non-existent in the very short endurance tests. The proportions of primary, secondary and tertiary creep were thus dependent upon the applied stress level and fracture type (as in static creep). The strain/time records of the 7 c/hr and 10 c/min tests were of the same general form and differed very little over the stress range tested. The low frequency tests underwent greater deformation during the first loading cycle by virtue of the lower elastic limit (Figures 8.1 and 8.3). The 7 c/hr tests were rather restricted in such comparisons however because there were no brittle type fractures obtained from tests of up to 143 hr duration. The diametral extensometer was of course sited at the mid-gauge length and fractures usually occurred above or below this position. The recorded strain was thus generally characteristic of the uniform deformation, and, unlike elongation records, did not necessarily include the additional local strain where the specimens necked down prior to fracture. It appeared that the cyclic strain range increased very slightly during the primary and tertiary stages of the tests.

### 9.2 Push/pull strain records

The strain records of push/pull tests were more varied in character and appeared to be even more dependent on testing conditions than those of the repeated tension tests. The strains could be defined in terms of primary, secondary and tertiary stages although these were rather confused in some of the very low endurance records. The secondary steady state stage appeared to be almost entirely absent in the low endurance tests (as was the case for repeated tension tests) and was evident in increasing proportions in the tests at lower applied stresses (Figures 8.2 and 8.4). The total accumulated strain of the high stress tests appeared to reach a more or less constant value during the initial stages, but in some cases increased in a compressive sense prior to fracture. The cyclic strain range generally increased during the primary deformation and either became constant prior to fracture or decreased again during the final stage. During lower stress tests, the general trend appeared to be for the total accumulated strain to increase slowly in a tensile direction during the primary stage, and remain constant during the secondary stage (as for repeated tension loading). The low frequency test records were markedly different from those of the high frequency type in that the strain ranges at comparable stresses were appreciably wider during the initial stages of the low frequency tests and increased at a greater rate during the subsequent life to failure e.g., the strain range of a 10 c/min test at ±60.4 ton/in$^2$ increased from an initial value of 0.32 to 0.71 per cent diametral strain immediately prior to fracture whereas a slower test (7 c/hr) at ±59.5 ton/in$^2$ increased from 0.43 to 1.64 per cent diametral strain.

In short, push/pull strain-time records exhibited cumulative creep in a compressive direction at high stresses and either remained constant or crept in a tensile direction at lower stresses. Low frequency tests exhibited greater cyclic strain ranges than did high frequency tests, and the range increased at a greater rate during the test life (of 7 c/hr tests as opposed to 10 c/min tests).

## 10.0 Discussion

A surprising feature of the behaviour of the H46 steel was the presence of regions of intercrystalline fracture even in the static half cycle case. Whilst none of the fatigue fractures examined were found to be either fully transcrystalline or fully intercrystalline, there appeared to be a large number of small intercrystalline cracks both adjacent to and remote from all the fracture surfaces. The brittle type failures contained the largest proportion of intercrystalline fracture paths whilst the ductile failures had deep fissures parallel to the test direction which were themselves mostly intercrystalline. The common feature in both types of fatigue fracture appeared to be the presence of intercrystalline sub-cracks of apparently random orientation behind the main fracture path. It is possible that these were initiated during the secondary fatigue stage, and that the final separation mechanism was either of a ductile or brittle type, depending upon whether the micro-cracks reached a critical size and distribution. If this was the case, then the initiations of both failures were similar but the final separation mechanisms differed. This possibility is supported by the strain-time records taken in the region of uniform deformation to the extent that there was primary, secondary, and some tertiary stage deformation, for both types of fractures and the chief difference between the fracture types as measured by the records was the amount of tertiary deformation prior to fracture. The visual appearance of the ductile fractures was very suggestive of shear failure on (110) planes through severely deformed material. Apart from the previously mentioned fissures and areas of intercrystalline separation, their appearance was typical of static room temperature fractures. On the other hand the appearance of the brittle type fractures was suggestive of cleavage but this was unsubstantiated by any more positive tests. The changeover from a ductile to a brittle fracture appearance was similar to that occurring in static ductile-brittle transition temperature tests.

The repeated tension test results (Figure 2) suggested that the fracture appearance changed at a critical number of cycles and applied stress of around $10^4$ cycles and 69 ton/in$^2$. There was little or no such evidence in the push/pull test data (Figure 3) and a critical fracture changeover condition was either non-existent for push/pull loading in terms of applied stress, number of cycles to failure and S/N slope, or was peculiar to repeated tensile fatigue.

In the past, considerable attention has been given to the slopes of the S/N or S/t curves derived from fatigue tests. Unfortunately, low cycle constant load amplitude fatigue differs from rapid conventional fatigue in that both stress and strain vary during the life to failure, and the nominal applied stress is relevant to the first setting up cycle only and is not necessarily related to the steady state condition reached during secondary stage fatigue. This argument does not apply to high frequency fatigue such as the 8000 c/min tests however, because under rapid loading conditions, the deformation is predominantly elastic, and there is negligible creep during the life to failure. The maximum nominal stress is thus no different from true stress since the cross-section and load remain virtually unchanged. Unfortunately the inherent scatter of the 8000 c/min fatigue tests was significantly greater than that at the lower frequencies and it was difficult to make a detailed analysis of the data. Despite these reservations a number of points of interest do arise from the results. The repeated tension tests have S/N curves that appear to belong to two definite regimes; a high stress, low cycle regime with a very low slope, and a lower stress regime with a higher slope at numbers of cycles exceeding about 5000. The transition between these two regimes may be associated with the observed change in the type of fracture, or alternatively the changeover may be peculiar to the testing ranges available. A second point of interest is that the push/pull data for the three frequencies can be fitted by similar S/N curves with some suggestion that the overall shape is sigmoidal. These curves exhibited only one regime, and this was similar to the steep portion of the S/N curves for the repeated tension tests. The brittle type push/pull fractures were at stresses below 61 ton/in$^2$ but showed no marked departure from the general trend of results.

The ultimate tensile stresses at loading rates corresponding to the 7 c/hr and 10 c/min frequencies (18 and 140 ton/in$^2$/min) could be joined smoothly to the two respective S/N fatigue curves for both repeated tension and push/pull loading. The difference in the values of U.T.S. at the respective loading rates was equal to the stress-wise separation of the fatigue curves. Thus, if the U.T.S./speed dependency together with the general shape of the S/N curves are known, a family of curves can be plotted for the range 7 c/hr to 8000 c/min. The long term prediction into the conventional fatigue range is a separate problem since the fatigue endurance limit was not reached during these tests, and if the cycle dependency remained operative for the lowest frequency (7 c/hr) tests, the limit would not be expected to be reached before $10^6$ cycles i.e., 16 years!

Differences between a unidirectional fatigue test and a reversed stress condition can often be ascribed to the Bauschinger effect. This was well illustrated by the repeated tension and push/pull strain-time records made during the two types of test (Figures 9.2 and 9.3). The specimens subjected to fast and slow frequency repeated tension tests work hardened during the initial cycles and reached a steady stage quasi-elastic condition during the secondary stage. On the other hand, the materials subjected to high stress push/pull cycles softened during each reversal and did not reach a work hardened elastic condition. This then suggests a possible explanation for the increase in the push/pull cyclic strain range during high stress reversals on the basis that the softening effect during a reversal exceeds the hardening during loading. The work hardening and softening effects appeared to cancel out at the lower stresses because a comparatively steady state secondary stage was reached during a fast test at ±50.0 ton/in$^2$ and the ultimate fracture was brittle type. The tendency for the strain range or amplitude to decrease during the tertiary stage of some of the high stress push/pull tests may be due to a delayed hardening mechanism or to an instability effect prior to fracture associated with either an onset of non-axial loading or with fracture instability. Another facet of the Bauschinger effect was the increase in cyclic strain range during the 7 c/hr tests compared with that of the 10 c/min tests at nominally equal stress ranges. Again, this is almost certainly caused by the enlargement of the elastic range with decrease in loading rate which in turn decreases the plastic strain per cycle and reduces the magnitude of the Bauschinger effect. This was not observed in repeated tension tests beyond the first few work hardening cycles after which the material settled down to an effectively elastic state which was independent of the loading rate. The fact that at a given stress level the slower loading rates gave shorter endurances, may be due to the additional plastic strain being itself more damaging to the material. Similarly, the decreased endurance in push/pull loading tests compared with repeated tension tests loaded to the same maximum nominal stress, may also be caused by the increased proportions of plastic strain present. Clearly these considerations do not apply to the 8000 c/min elastic type tests where there is virtually no plastic strain involved.

The S/t repeated tension diagram (Figure 1) is of particular interest since it illustrates a 'cross-over point' (at 70.5 ton/in$^2$ and 5.75 hr to failure) on the 7 c/hr and 10 c/min curves. The region to the left is governed by a creep type condition in the sense that higher frequency tests exhibit longer durations in hours, and the cross-over point itself is the condition where time to failure is independent of the two applied frequencies. The region to the right of the point approximates to the normal fatigue condition; with increasing life the number of cycles to failure becomes more nearly constant and is independent of applied frequency. If the conditions to give a life to failure of 1 hr are considered from Figure 1, it is evident that the order of increasing strength is 8000 c/min, 7 c/hr, 10 c/min - an anomalous effect also noted for Nimonic 90 at elevated temperatures[1]. The low stress end of the 10 c/min curve approached the 8000 c/min curve such that this region also approximated to a time dependent failure condition independent of the two frequencies. The push/pull test curves exhibited no 'cross-overs' and it is clear that only the repeated tension fatigue was time dependent at high stresses. The push/pull and repeated tension S/N curves at a given applied frequency converged towards the U.T.S. value (at that loading rate) such that the high stress, low endurance, conditions exhibited less differences between the respective lives than did low stress conditions i.e., endurance appeared to be related to the maximum applied stress. Conversely, the two S/N curves diverged with decreasing maximum applied stress to the point where the range of stress rather than the maximum applied stress determined failure.

## 11.0 Conclusions

(i) Ductile-type fractures were observed at very high stresses close to the U.T.S. and brittle type fractures were evident at lower stresses. Both types of fractures appeared to have been preceded by intercrystalline cracking and the final fracture paths contained mixed areas of intercrystalline and transcrystalline separation. The proportion of intercrystalline separation appeared to be greatest in the brittle type fractures. Fatigue-like regions were observed on some of the longer time brittle type failures.

(ii) The ductile fractures of the repeated tension tests appeared to be associated with very high stress fatigue at less than 5000 cycles to failure whereas the brittle type fractures were associated with lower stresses and greater numbers of cycles to failure. There was a marked increase in slope of the stress/endurance (S/N) curve at the fracture changeover point.

(iii) The changeover in fracture type of the push/pull test specimens did not coincide with either a change in slope of the S/N curve or with a particular endurance value for the three respective applied frequencies.

(iv) The higher frequency fatigue tests gave longer endurances in terms of cycles to failure for all types of applied loading.

(v) For a given applied frequency, the push/pull and repeated tension curves converged with increasing stresses to the ultimate tensile strength. In the case of repeated tension, the stress/time (S/t) curves at 7 c/hr and 10 c/min crossed over such that the condition to the left of the cross-over was virtually time-dependent, and that to the right tended to a cycle-dependence with increasing number of cycles. The stress-wise separation of the S/N curves was approximately equal to the difference in static U.T.S.'s at the corresponding loading rates.

(vi) The enlarged cyclic strain amplitude of the push/pull and slow frequency tests as opposed to repeated tension and higher frequency tests, has been tentatively explained in terms of the Bauschinger effect.

ACKNOWLEDGEMENTS

The author gratefully acknowledges many helpful discussions with Mr. A. Graham together with his permission to test the H46 steel and expresses his thanks to Mr. W. Gwenlan for setting up the fatigue tests and mounting the metallographic sections, to Mr. J. E. Northwood for supervising the metallographic preparations and photographs and to Mr. G. J. Bates for carrying out the heat treatment and hardness tests on the H46 alloy.

## NOTATION

| | |
|---|---|
| S | The nominal maximum applied stress per cycle |
| N | Number of fatigue cycles to failure |
| t | The time to failure |
| U.T.S. | Ultimate Tensile Strength |

## REFERENCES


| No. | Author(s) | Title |
|---|---|---|
| 1 | G. P. Tilly | Effects of varied loading paths on fatigue endurances, Part I - Some load fatigue properties of Nimonic 90 at elevated temperatures. A.R.C. C.P.786. December, 1963. |
| 2 | N. Stephenson<br>J. E. Northwood<br>R. S. Smith | The effects of alternating stress at elevated temperatures on structural changes in Nimonic 90. N.G.T.E. Memorandum No. M.325. July, 1959. |
| 3 | W. A. Wood | Some basic studies in the fatigue of metals, fracture. April, 1959. Edited by Auerbach et al. |
| 4 | C. S. Landau | Low frequency fatigue of Nimonic 90 N.G.T.E. Report No.R.243. September, 1960. A.R.C.22 309. |

# TABLE I

## Constant load amplitude fatigue test results on H46 steel at room temperature

### Repeated tension tests

| Nominal frequency | Maximum applied stress (ton/in$^2$) | Cycles to failure | Life (hr) | Fracture type |
|---|---|---|---|---|
| c/hr | 70.5 | $\frac{1}{2}$ | 0.159 | Ductile |
| | 69.4 | 50 | 6.15 | Ductile |
| | 68.5 | 830 | 97.9 | Cracked/Unbroken |
| | 68.8 | 1210 | 143.1 | Cracked/Unbroken |
| | 70.0 | 47 | 5.75 | Ductile |
| 10 c/min | 72.5 | $\frac{1}{2}$ | 0.00139 | Ductile |
| | 71.2 | 282 | 0.315 | Ductile |
| | 68.0 | 9709 | 9.6 | Brittle |
| | 70.3 | 5518 | 5.65 | Brittle |
| | 67.3 | 10620 | 10.6 | Brittle |
| | 65.0 | 12590 | 11.7 | Fatigue/Brittle |
| | 63.1 | 38736 | 34.8 | Fatigue/Brittle |
| | 61.3 | 72254 | 25.9 | Fatigue/Brittle |
| | 59.6 | 26723 | 56.0 | Fatigue/Brittle |
| 8000 c/min | 69.3 | $10 \times 10^3$ | 0.021 | Ductile |
| | 68.0 | $12 \times 10^3$ | 0.025 | Ductile |
| | 65.3 | $38 \times 10^3$ | 0.078 | Brittle |
| | 61.3 | $815 \times 10^3$ | 1.7 | Brittle |
| | 58.9 | $342 \times 10^3$ | 0.8 | Brittle |
| | 57.2 | $63118 \times 10^3$ | 113.1 | Fatigue/Brittle |

TABLE I (cont'd)

Push/Pull Tests

| Nominal frequency | Maximum applied stress (ton/in$^2$) | Cycles to failure | Life (hr) | Fracture type |
|---|---|---|---|---|
| 7 c/hr | 69.8 | 3 | 0.8 | Ductile |
| | 66.0 | 10 | 3.2 | Ductile |
| | 63.8 | 32 | 8.0 | Ductile |
| | 59.5 | 276 | 61.9 | Ductile |
| 10 c/min | 71.2 | 4 | 0.0128 | Ductile |
| | 68.7 | 10 | 0.0485 | Ductile |
| | 65.0 | 52 | 0.13 | Ductile |
| | 60.4 | 397 | 0.7 | Fatigue/Brittle |
| | 55.0 | 1151 | 1.9 | Brittle |
| | 50.0 | 9907 | 15.5 | Fatigue/Brittle |
| | 43.5 | 42038 | 58.8 | Shear |
| | 58.0 | 919 | 1.55 | Fatigue/Brittle |
| | 53.0 | 4618 | 7.7 | Shear |
| | 60.2 | 458 | 0.9 | Fatigue/Brittle |
| 8000 c/min | 47.6 | $13 \times 10^3$ | 0.0001 | Cracked/Unbroken |
| | 45.0 | $95 \times 10^3$ | 0.166 | Cracked/Unbroken |
| | 41.3 | $495 \times 10^3$ | 1.1 | Failed outside test section |
| | 41.3 | $162 \times 10^3$ | 0.35 | Cracked/Unbroken |
| | 38.6 | $49050 \times 10^3$ | 107.6 | Fatigue/Brittle |

# APPENDIX I

## The diametral extensometer

### (i) Diametral strain measurements during low cycle fatigue

Strain measurements during uniaxial material testing are usually made on the specimen gauge length and expressed as elongations. Diametral recordings are an alternative measure that can be useful in situations where the transverse strain is particularly required or where the geometry and installation of the specimen favours diametral gauges. Slow-speed tests on the Amsler Vibrophore testing machine require specimens with short gauge lengths to reduce buckling effects during compression and leave very little space to site extensometer apparatus. The room temperature tests are particularly cramped since there is only $1\frac{1}{4}$ in. between the upper and lower machine grips when the specimen is set up. Diametral deformations are small compared to the elongations of standard type specimens and if similar measuring apparatus were used then diametral recordings would be less accurate than their longitudinal counterparts by a factor determined by the ratio of diameter to gauge length and Poisson's ratio. Fortunately commercial electronic gauging apparatus has been developed to the extent that deformations of 0.00001 in. can be measured; however, it is the larger deformations that present difficulties since they cannot be contained within the linear range of this type of equipment. It is under these conditions that diametral type extensometers can be used very conveniently with high accuracy electronic gauges whereas longitudinal instruments present special difficulties.

During uniform deformation of the specimen the longitudinal and transverse strains are related by Poisson's ratio, but during the final stages prior to a low cycle fatigue fracture localised deformation takes place and both measures are adversely affected. The necked region is usually contained by the gauge length and the longitudinal strain is an averaged value of the uniform and localised regions. In the case of the diametral measurement this usually continues to record the uniform deformation unless it happens to be sited at the region of localised deformation and eventual fracture.

### (ii) The room temperature diametral extensometer

A gauging assembly was suspended on leaf springs such that a knife edge was located one side of the test-piece diameter and a differential transformer type probe followed the deformation at a point diametrically opposite (Figure 10.1). The leaf springs were arranged so as to be flexible in two dimensions and rigid in the third. Vertical leaves were employed to load the knife edge against the test-piece and ensure that it remained in true contact throughout the test (Figure 10.2). Horizontal leaves were arranged to suspend the unit and at the same time allow it to deflect with the specimen in a longitudinal direction and ensure that the knife edge did not slip during longitudinal deformation. The system was rigid in the third dimension and ensured that a line drawn through the centreline of the probe and knife edge assembly always passed through the centre of the specimen. The probe was based on a differential transformer principle and was arranged such that the deflection of a moving coil core produced a signal that was fed to a gauge unit and strip chart recorder. The core was sprung by a 2 oz helical spring such that maximum deflection was recorded in the unloaded "out" position. During the setting up of a test the probe was loaded against the specimen and the core was pushed back into the probe by use of a micrometer screw head. The micrometer was used for calibration and for adjustment of the gauge to zero deflection at the beginning of a test. For a tensile deformation of the specimen the diameter is decreased, the core is pushed out of the probe by the 2 oz spring and a positive deformation is recorded on the instrument. For compressive deformation the core is pushed further into the probe and negative deformation is recorded. The linear ranges of the instrument were ±0.0005 in. and ±0.005 inch. If for some reason the maximum range was exceeded during a test, the record could be reset to zero by the micrometer and the test continued.

D 31137/1/R.54 400 1/65 R

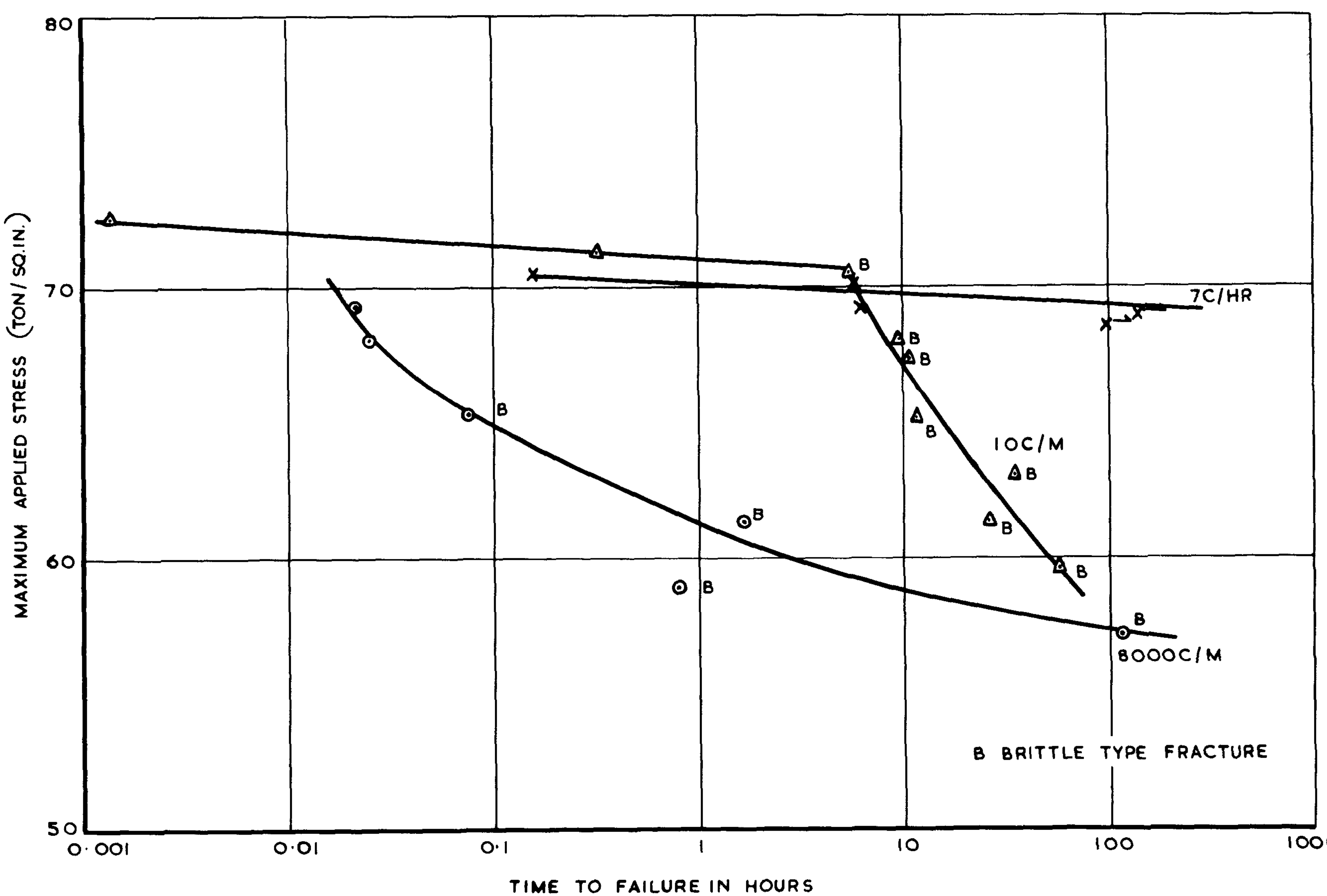


FIG.1

CONSTANT LOAD AMPLITUDE
ROOM TEMPERATURE FATIGUE TESTS ON H46:
REPEATED TENSION.

FIG. 2

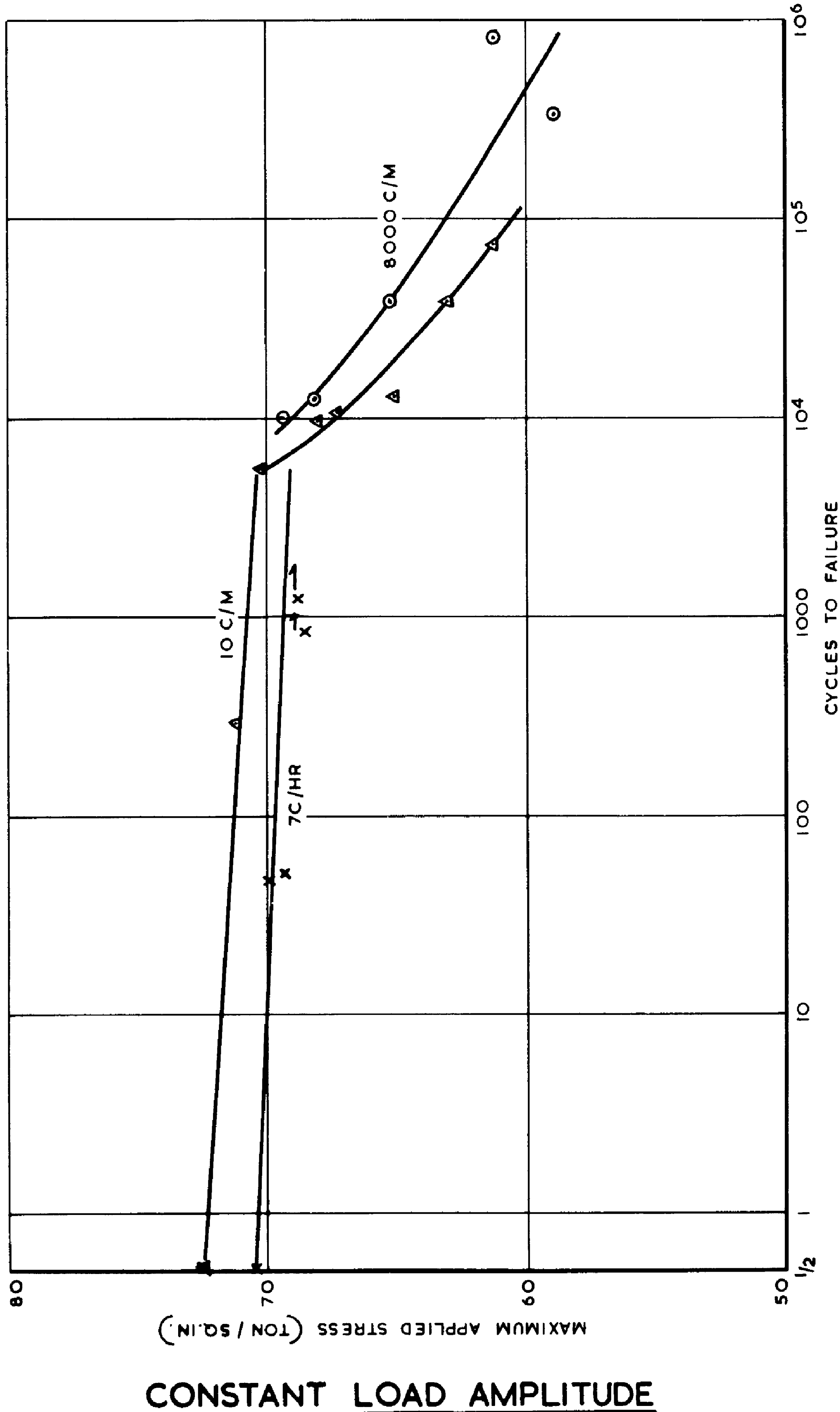


CONSTANT LOAD AMPLITUDE

ROOM TEMPERATURE FATIGUE TESTS ON H46:

REPEATED TENSION.

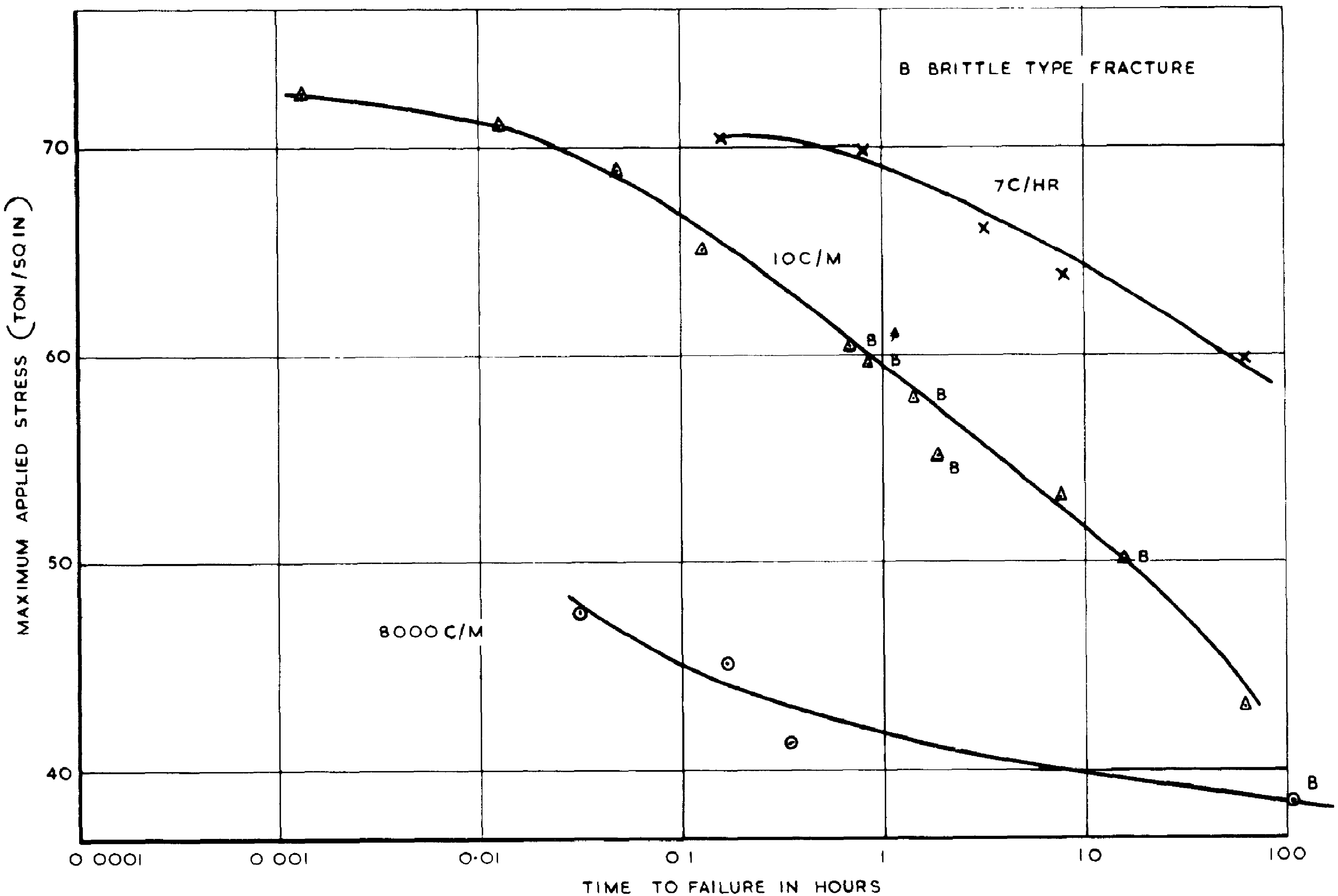


FIG. 3

ROOM TEMPERATURE FATIGUE TESTS ON H46:

CONSTANT LOAD AMPLITUDE

PUSH / PULL.

FIG. 4

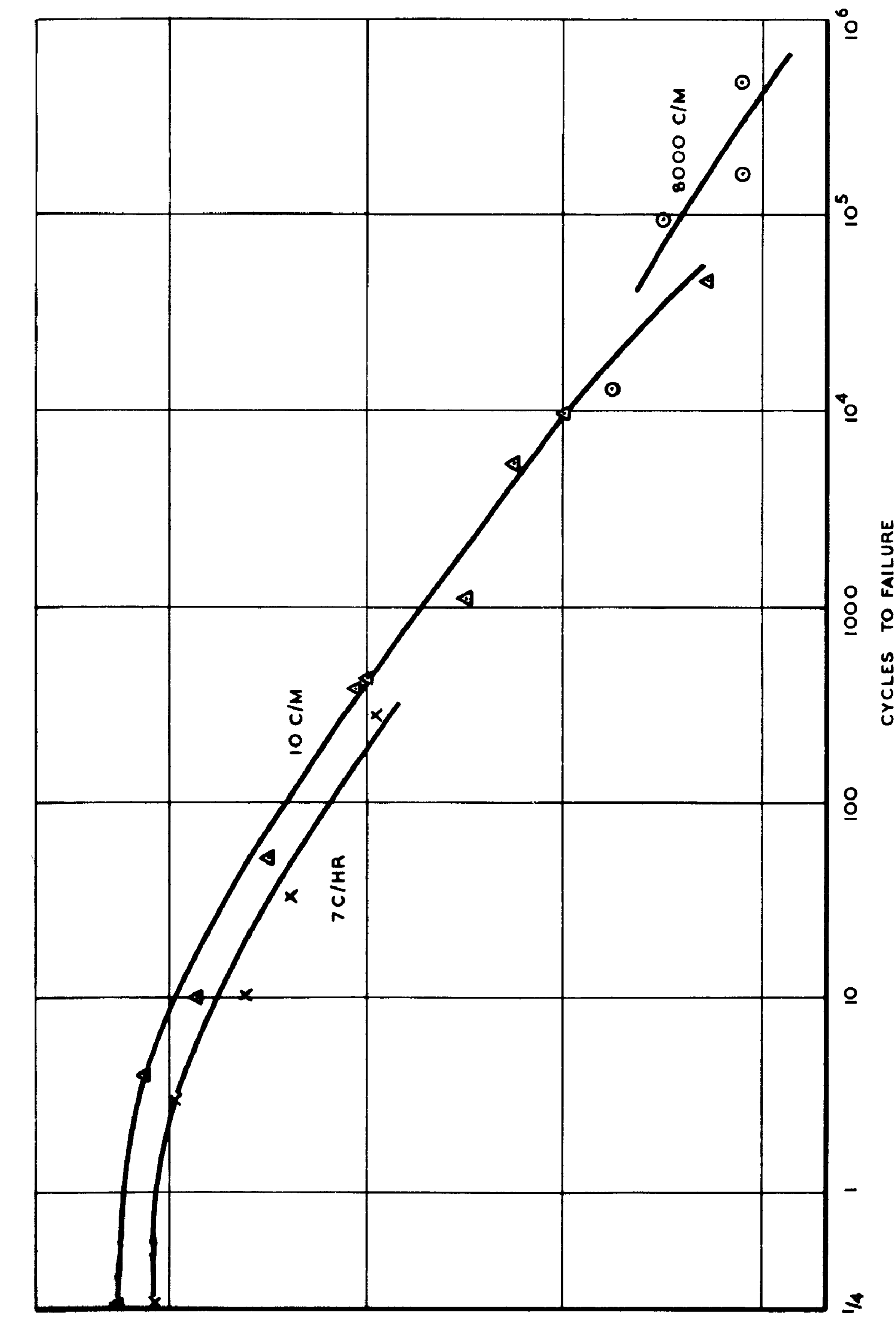


**CONSTANT LOAD AMPLITUDE**
**ROOM TEMPERATURE FATIGUE TESTS ON H 46:**
**PUSH/PULL**

FIG.5.

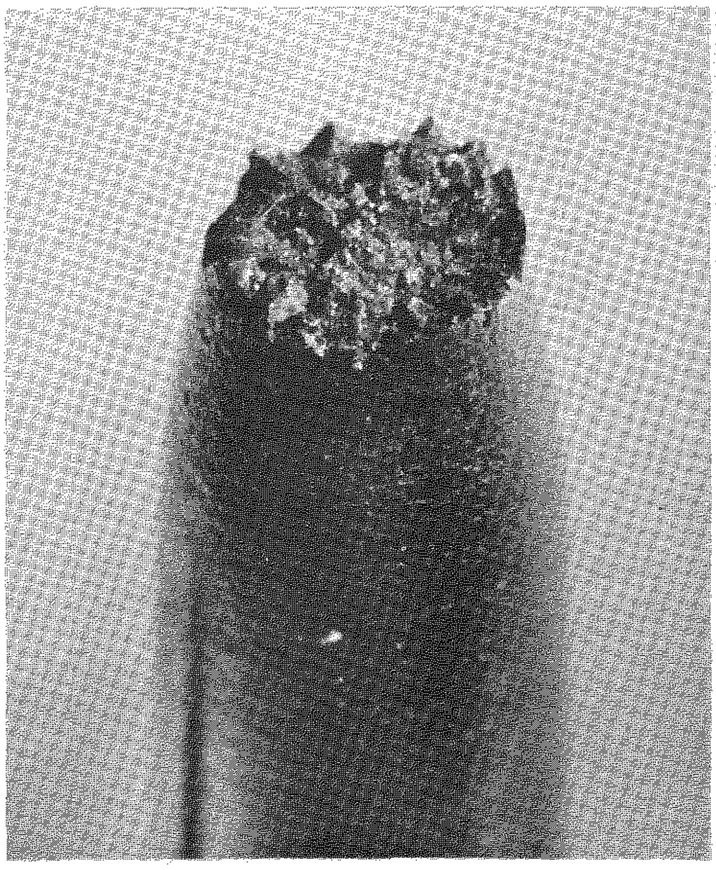

5·1 A TYPICAL DUCTILE TYPE FRACTURE OF H46 STEEL AT ROOM TEMPERATURE

MAG X 15

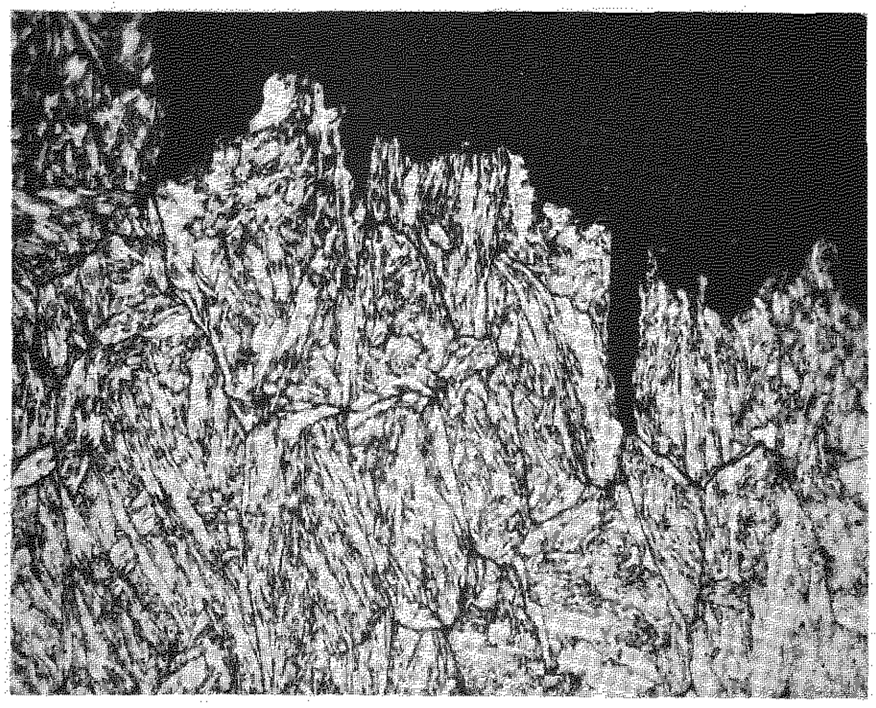

5·2 A SECTION TAKEN PERPENDICULAR TO THE DUCTILE FRACTURE SURFACE AND ETCHED WITH A 10% AMMONIUM PERSULPHATE SOLUTION. THE FISSURE ON THE RIGHT HAND SIDE APPEARS TO LEAD INTO A REGION OF INTER-CRYSTALLINE SEPARATION WHILST THE MAIN TRANS-CRYSTALLINE FRACTURE PATH PASSES THROUGH HEAVILY DEFORMED MATERIAL.

MAG X 500

FIG.6.

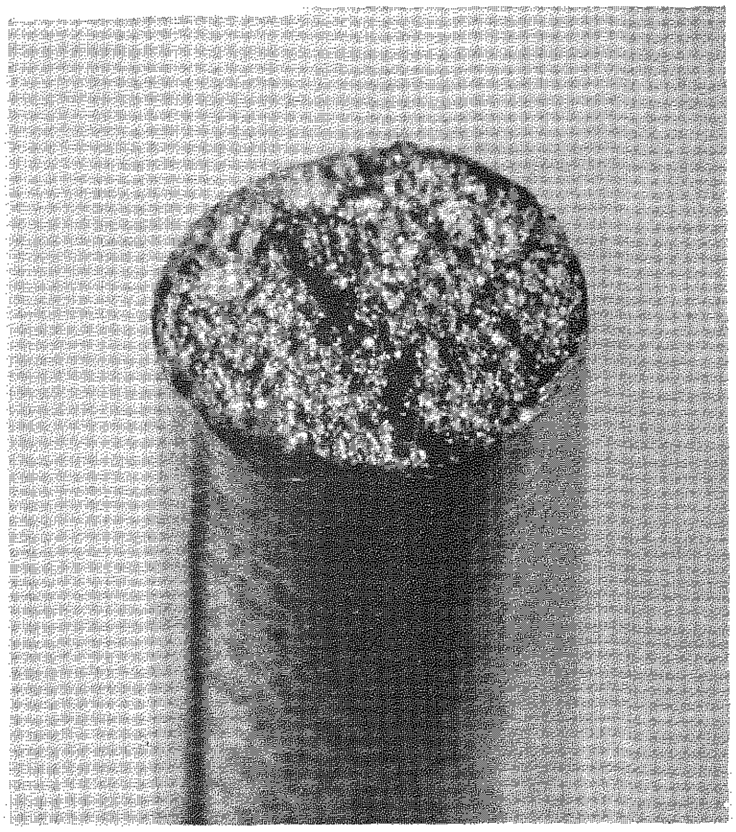

6·1 A TYPICAL BRITTLE TYPE FRACTURE OF H 46 STEEL AT ROOM TEMPERATURE.

MAG X 15

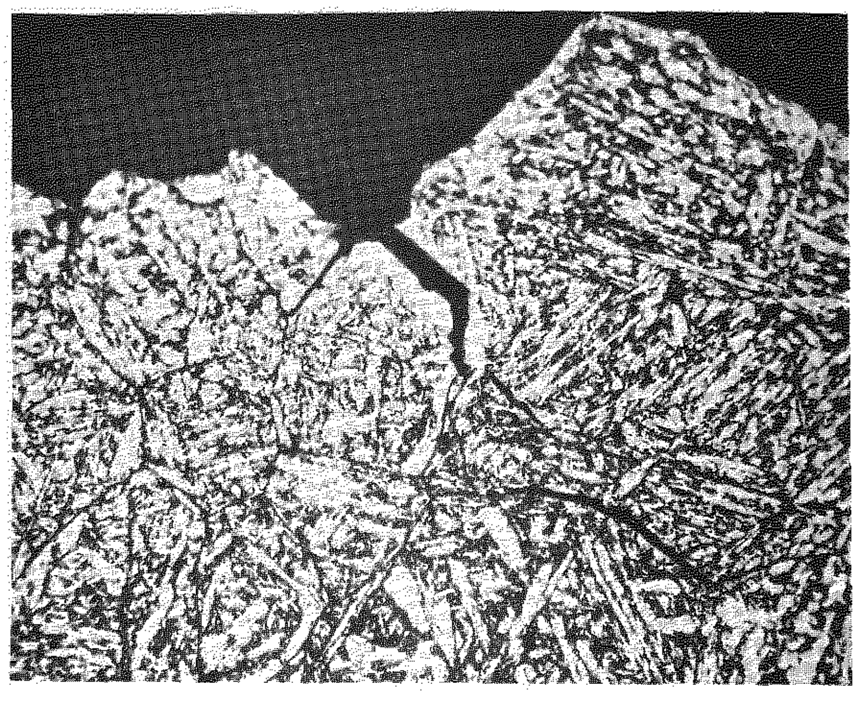

6·2 A SECTION TAKEN PERPENDICULAR TO THE BRITTLE FRACTURE SURFACE AND ETCHED WITH A 10% AMMONIUM PERSULPHATE SOLUTION. THE TRANS CRYSTALLINE FRACTURE PATH PASSES THROUGH VIRTUALLY UNDEFORMED GRAINS AND THERE IS SOME INTER CRYSTALLINE SEPARATION IN THE BOTTOM LEFT HAND CORNER.

MAG X 500.

FIG.7.

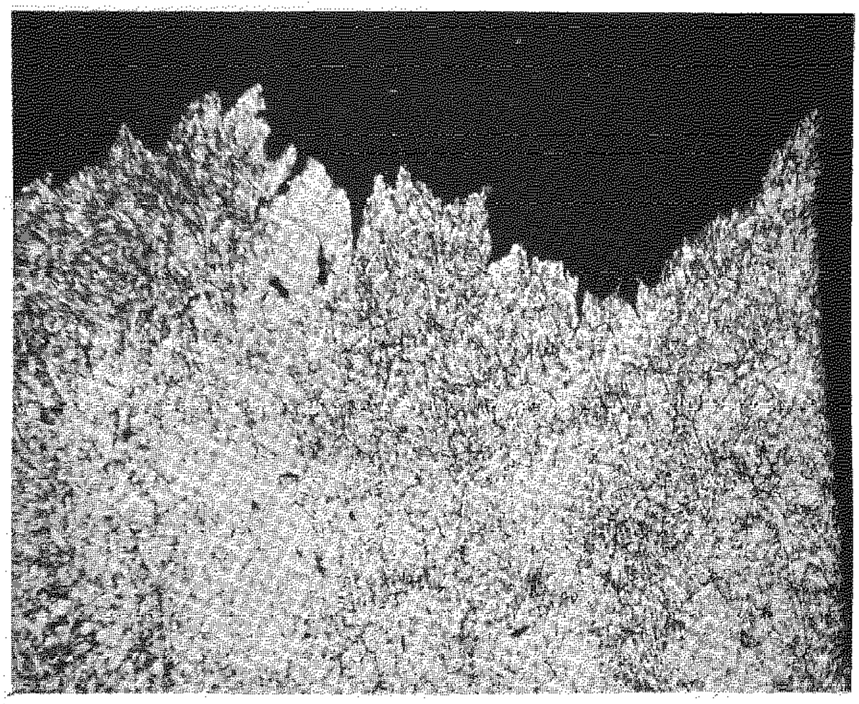

7·1 ETCHED SECTION TAKEN PERPENDICULAR TO A DUCTILE FRACTURE SURFACE TO ILLUSTRATE THE PRESENCE OF THE INTER-CRYSTALLINE CRACKS IN THE MATERIAL BEHIND THE FRACTURE PATH.

MAG X 100

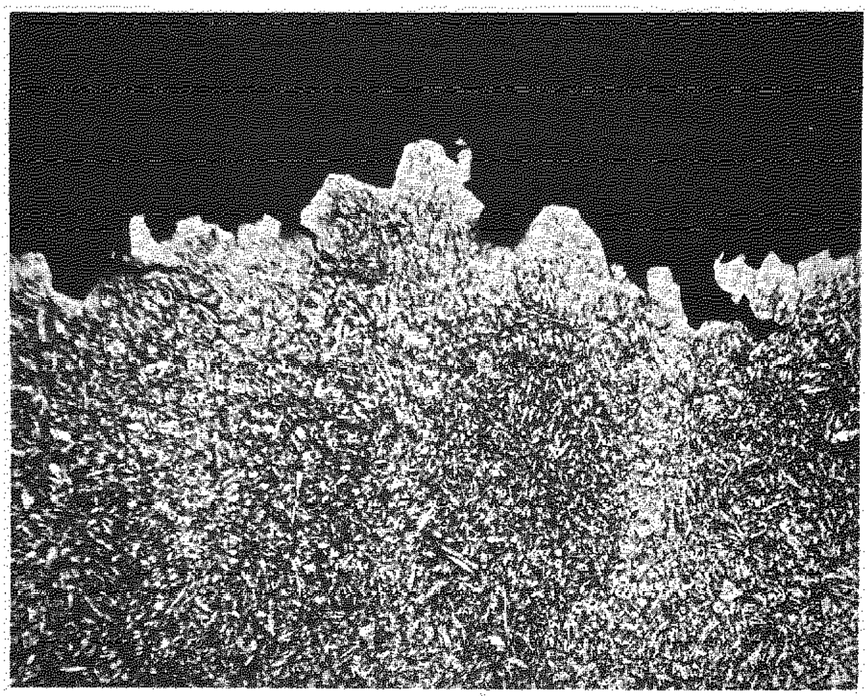

7·2 ETCHED SECTION TAKEN PERPENDICULAR TO A BRITTLE FRACTURE SURFACE TO ILLUSTRATE THE MIXED INTER-AND TRANS - CRYSTALLINE SEPARATION.

MAG X 100

FIG.8

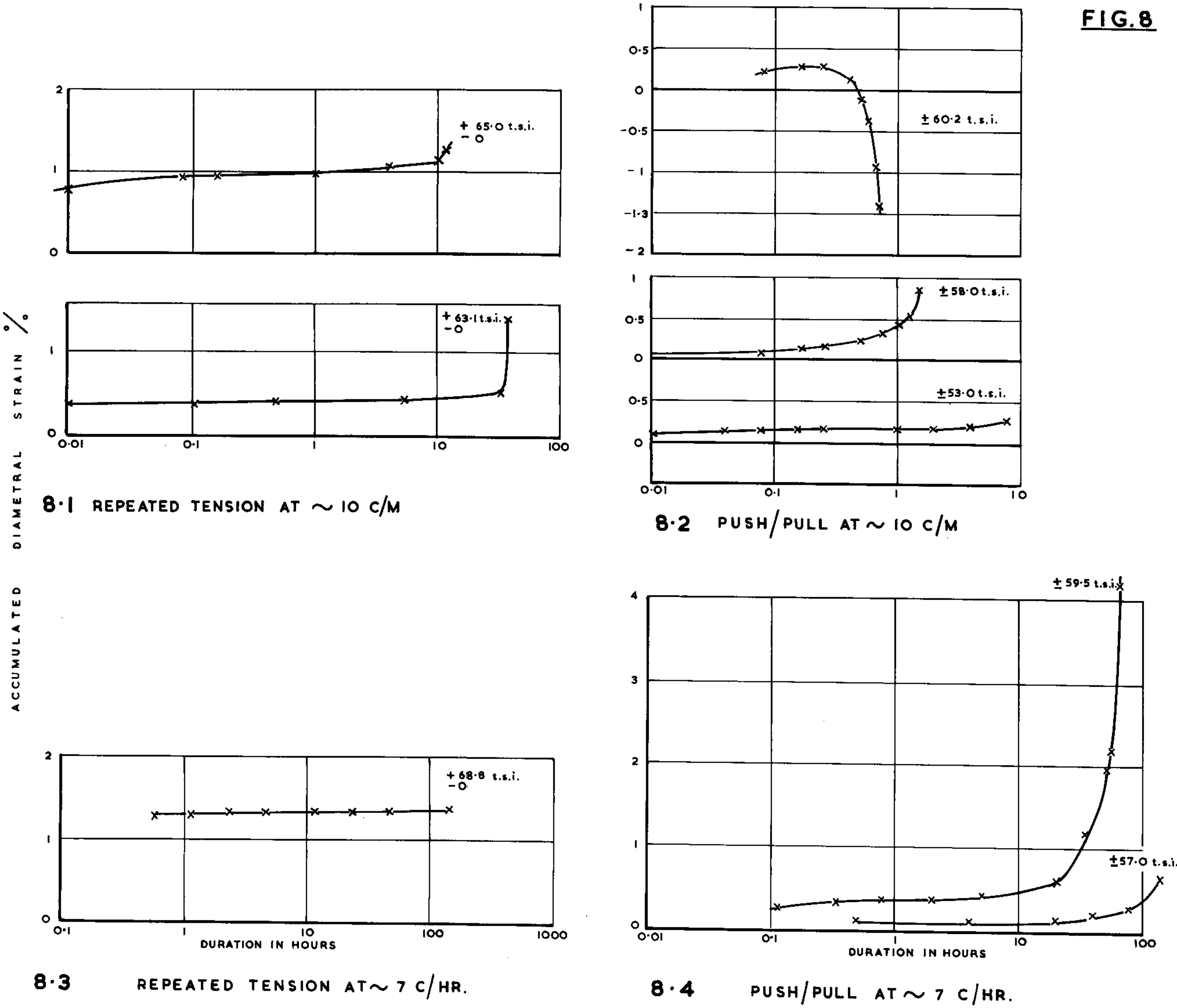


CUMULATIVE STRAIN/TIME CURVES FOR ROOM TEMPERATURE FATIGUE OF H.46.

FIG. 10

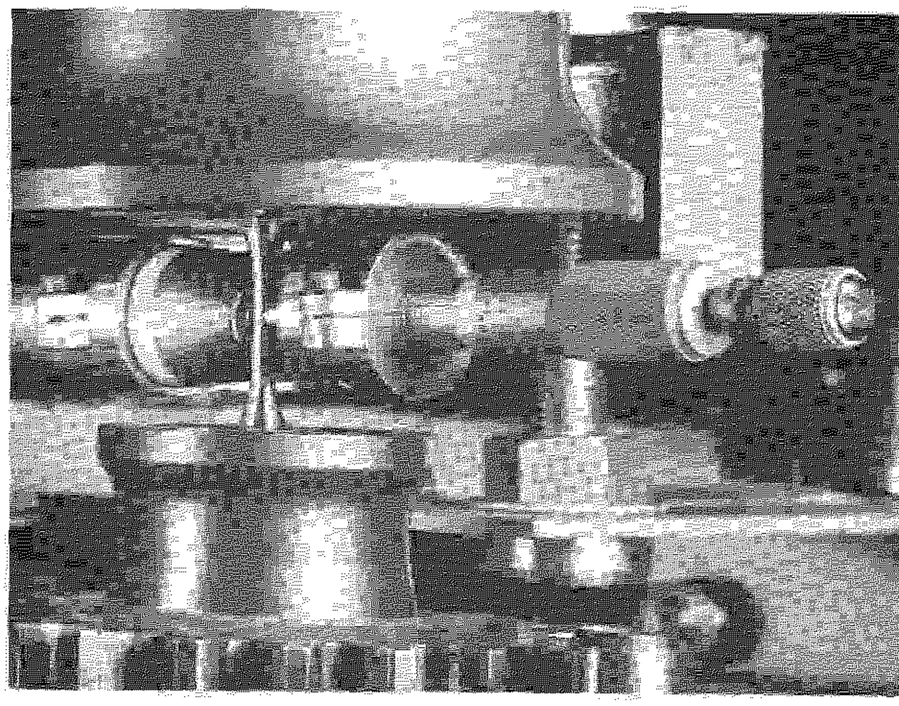

10·1 FRONT VIEW OF THE DIAMETRAL EXTENSOMETER

THE PROBE TIP AND KNIFE EDGE ARE LOCATED AT DIAMETRICALLY OPPOSITE POINTS ON THE TEST-PIECE. CALIBRATION AND ADJUSTMENT ARE MADE WITH THE MICROMETER HEAD

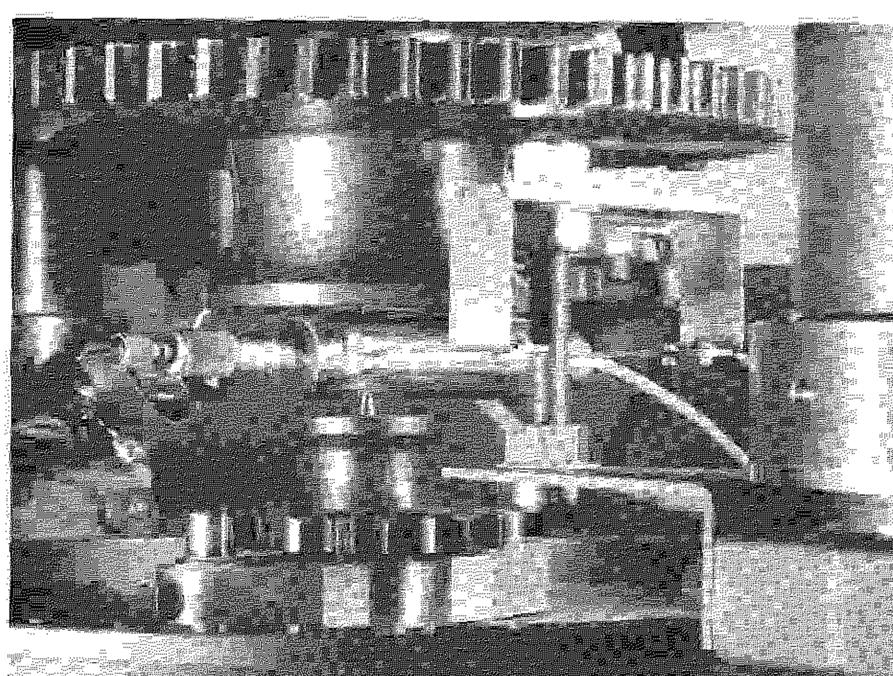

10·2 REAR VIEW OF THE EXTENSOMETER

THE UNIT CONTAINING THE PROBE AND MICROMETER IS SUSPENDED BY VERTICAL AND HORIZONTAL LEAF SPRINGS

A.R.C. C.P. No. 787 539.431:669.15-194.57
March, 1964
Tilly, G. P.

EFFECTS OF VARIED LOADING PATHS ON FATIGUE ENDURANCES
PART II - SOME LOAD FATIGUE PROPERTIES OF H46
AT ROOM TEMPERATURE


The constant load amplitude fatigue properties of an 11 per cent Cr-Mo-V-Nb steel (H46), have been examined at frequencies of 7 c/hr, 10 c/min and 8000 c/min at room temperature for repeated tension and push/pull loading.

Ductile type fractures were observed at very high stresses and brittle type fractures at less high stresses. The fracture types contained regions of both intercrystalline and transcrystalline failure together with numerous intercrystalline sub-cracks behind the fractures. The push/pull and the repeated tension stress/cycles to failure (S/N)


P.T.O.

A.R.C. C.P. No. 787 539.431:669.15-194.57
March, 1964
Tilly, G. P.

EFFECTS OF VARIED LOADING PATHS ON FATIGUE ENDURANCES
PART II - SOME LOAD FATIGUE PROPERTIES OF H46
AT ROOM TEMPERATURE

The constant load amplitude fatigue properties of an 11 per cent Cr-Mo-V-Nb steel (H46), have been examined at frequencies of 7 c/hr, 10 c/min and 8000 c/min at room temperature for repeated tension and push/pull loading.

Ductile type fractures were observed at very high stresses and brittle type fractures at less high stresses. The fracture types contained regions of both intercrystalline and transcrystalline failure together with numerous intercrystalline sub-cracks behind the fractures. The push/pull and the repeated tension stress/cycles to failure (S/N)

P.T.O.

A.R.C. C.P. No. 787 539.431:669.15-194.57
March, 1964
Tilly, G. P.

EFFECTS OF VARIED LOADING PATHS ON FATIGUE ENDURANCES
PART II - SOME LOAD FATIGUE PROPERTIES OF H46
AT ROOM TEMPERATURE

The constant load amplitude fatigue properties of an 11 per cent Cr-Mo-V-Nb steel (H46), have been examined at frequencies of 7 c/hr, 10 c/min and 8000 c/min at room temperature for repeated tension and push/pull loading.

Ductile type fractures were observed at very high stresses and brittle type fractures at less high stresses. The fracture types contained regions of both intercrystalline and transcrystalline failure together with numerous intercrystalline sub-cracks behind the fractures. The push/pull and the repeated tension stress/cycles to failure (S/N)

P.T.O.

fatigue curves converged to the static ultimate tensile strength at high stresses. Variations in the cyclic strain ranges of the different tests were examined and discussed in terms of the Bauschinger effect. The very high stress repeated tension tests at frequencies of 7 c/hr and 10 c/min exhibited a creep type time-dependent failure condition, whereas less high stresses tended to the more common room temperature cycle-dependent fatigue condition. For all testing conditions, the general trend was for higher frequencies to give greater numbers of cycles to failure at equivalent stresses and loading paths.

fatigue curves converged to the static ultimate tensile strength at high stresses. Variations in the cyclic strain ranges of the different tests were examined and discussed in terms of the Bauschinger effect. The very high stress repeated tension tests at frequencies of 7 c/hr and 10 c/min exhibited a creep type time-dependent failure condition, whereas less high stresses tended to the more common room temperature cycle-dependent fatigue condition. For all testing conditions, the general trend was for higher frequencies to give greater numbers of cycles to failure at equivalent stresses and loading paths.

fatigue curves converged to the static ultimate tensile strength at high stresses. Variations in the cyclic strain ranges of the different tests were examined and discussed in terms of the Bauschinger effect. The very high stress repeated tension tests at frequencies of 7 c/hr and 10 c/min exhibited a creep type time-dependent failure condition, whereas less high stresses tended to the more common room temperature cycle-dependent fatigue condition. For all testing conditions, the general trend was for higher frequencies to give greater numbers of cycles to failure at equivalent stresses and loading paths.

C.P. No. 787



Printed and published by
HER MAJESTY'S STATIONERY OFFICE
To be purchased from
York House, Kingsway, London w c 2
423 Oxford Street, London w 1
13A Castle Street, Edinburgh 2
109 St Mary Street, Cardiff
39 King Street, Manchester 2
50 Fairfax Street, Bristol 1
35 Smallbrook, Ringway, Birmingham 5
80 Chichester Street, Belfast 1
or through any bookseller

*Printed in England*

C.P. No. 787

S.O. Code No. 23-9015-87